MAGNETIC RESONANCE IN CHEMISTRY, VOL. 36, 39–45 (1998)

N-Triorganostannyl-Substituted Pyrroles and Indoles and *N*-Trimethylstannylcarbazole: Determination of Signs of Coupling Constants and Isotope-Induced Chemical Shifts $^{1}\Delta^{14/15}N(^{119}Sn)$

Bernd Wrackmeyer,* Gerald Kehr, Heidi E. Maisel and Hong Zhou

Laboratorium für Anorganische Chemie, Universität Bayreuth, D-95440 Bayreuth

Received 22 May 1997; accepted 31 July 1997

ABSTRACT: *N*-Triorganostannyl (R_3Sn)-substituted pyrroles (**1**) and indoles (**2**) [R = Me (**a**), Et (**b**), ^{t}Bu (**c**)], *N*-trimethylstannyl-carbazole (**3**), *N*-trimethylstannyl-2,5-dimethylpyrrole (**1d**), the corresponding silicon and lead derivatives [**1d(Si)** and **1d(Pb)**] and *N*-trimethylstannyl-2-methylindole (**2d**) were prepared and studied by multinuclear magnetic resonance (^{1}H, ^{13}C, ^{15}N, ^{29}Si, ^{119}Sn and ^{207}Pb NMR). The absolute signs of numerous coupling constants $^{n}J(^{119}Sn,^{13}C)$ and $^{1}J(^{119}Sn,^{15}N)$ (<0) were determined by appropriate 2D heteronuclear shift correlations of the type $^{13}C/^{1}H$ and $^{15}N/^{1}H$. Precise measurement of the coupling constants $^{1}J(^{119}Sn,^{15}N)$ from ^{119}Sn NMR spectra by using Hahn-echo extended (HEED) polarization transfer pulse sequences enabled one to obtain isotope-induced chemical shifts $^{1}\Delta^{14/15}N(^{119}Sn)$ at natural abundance of ^{15}N. The $^{1}\Delta^{14/15}N(^{119}Sn)$ data become more negative with increased branching of the substituent R at the tin atom and with stronger steric interactions. The latter effect is also evident from $\delta^{119}Sn$ values and changes in the magnitude of the coupling constants $^{1}J(^{119}Sn,^{13}C)$ or $^{1}J(^{119}Sn,^{15}N)$. © 1998 John Wiley & Sons, Ltd.

KEYWORDS: azoles; triorganotin; coupling constants; sign determination; isotope-induced chemical shifts

INTRODUCTION

Azoles bearing organometallic substituents are attractive reagents in synthesis owing to the reactive carbon– or nitrogen–element bonds. Although the Sn—N bond should be particularly reactive,[1] only a few *N*-stannylpyrazoles, -imidazoles, -triazoles and -pyrroles and *N*-trimethylstannylcarbazole have been prepared.[2–5] Systematic 1D ^{1}H, ^{13}C and ^{119}Sn NMR measurements have been carried out for some *N*-stannylpyrroles,[5,6] and 1D and 2D NMR techniques were applied to obtain ^{15}N NMR parameters for *N*-trimethylstannylpyrrole.[7] Our current interest in ^{15}N[8] and ^{119}Sn NMR parameters[9] prompted us to synthesize a series (Scheme 1) of *N*-triorganostannylpyrroles (**1**) and -indoles (**2**) and the carbazole derivative **3**. Coupling constants $^{1}J(^{119}Sn,^{15}N)$ for these compounds have not been reported, with the exception of **1a** and **1d**,[7] and this is also true for the signs of the coupling constants $^{n}J(^{119}Sn,^{13}C_{azole})$ and $^{n+1}J(^{119}Sn,^{1}H_{azole})$. These parameters will be discussed with respect to the different organyl groups attached to the tin atom and the nature of the azole system.

RESULTS AND DISCUSSION

The ^{13}C, ^{15}N and ^{119}Sn NMR data for compounds **1**–**3** are listed in Table 1. In general, there is reasonable agreement with literature data,[5–7] where available.

Measurement of $^{1}J(^{119}Sn,^{15}N)$ and isotope-induced chemical shifts $^{1}\Delta^{15/14}N(^{119}Sn)$

All values of $^{1}J(^{119}Sn,^{15}N)$ could be measured within a few minutes each from 1D ^{119}Sn NMR spectra by using

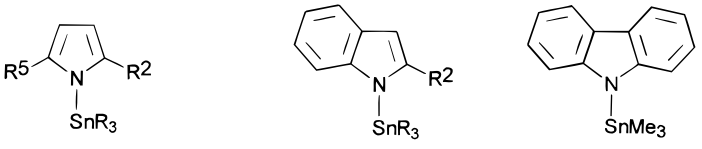

1	**a**	**b**	**c**	**d**	**e**	**f**
R	Me	Et	^{t}Bu	Me	Bz	Ph
$R^{2,5}$	H	H	H	Me	H	H

2	**a**	**b**	**c**	**d**
R	Me	Et	^{t}Bu	Me
R^{2}	H	H	H	Me

3

Scheme 1. N-Azolyltin compounds studied.

---

* *Correspondence to:* B. Wrackmeyer, Laboratorium für Anorganische Chemie, Universität Bayreuth, D-95440 Bayreuth, Germany.
Contract/grant sponsor: Deutsche Forschungsgemeinschaft.
Contract/grant sponsor: Fonds der Chemischen Industrie.

CCC 0749-1581/98/010039–07 $17.50

Table 1. ^{13}C, ^{15}N and ^{119}Sn (^{29}Si,^{207}Pb) NMR data[a] for *N*-pyrrolyltin derivatives **1a f**, the *N*-pyrrolylsilicon compound **1d(Si)** and the *N*-pyrrolyllead compound **1d(Pb)**

	δ^{13}C						
No.	C(2,5)	C(3,4)	R	R$^{2/5}$	δ^{119}Sn	$^1\Delta^{15/14}$N(^{119}Sn)[b]	δ^{15}N
1a	124.4	109.8	−3.8	—	72.9	−38.0	−216.2
	[−13.7]	[−16.4]	[−397.7]				[−37.2]
1b	125.0	109.8	5.0, 10.2	—	52.6	−48.0	−231.0
	[−9.0]	[−14.0]	[372.8] [26.2]				[66.5]
1c	125.6	109.9	32.7, 30.7	—	−9.2	−59.5	−222.9
	[−7.0]	[−12.9]	[389.6] [<2]				[−99.9]
1d	133.0	108.7	−3.4	16.5	57.2	−46.5	−216.1
	[−12.5]	[−19.6]	[−394.0]	[−7.1]			[−25.2]
1d(Si)	133.0	111.1	2.8	16.8	8.7[c]	−9.2[c]	−220.1[d]
	(<1.5)	(<1.5)	(−57.8)	(<1.5)			(13.5)
1d(Pb)	133.5	107.3	10.4	17.2	170.3[e]	−96.0[e]	−206.0
	{<5.0}	{<5.0}	{310.0}	{<5.0}			{300.1}
1e	124.9	109.7	21.4[f]	—	−29.1	−37.8	−219.7
	[−10.0]	[−15.7]	[323.0]				[89.1]
1f	126.3	110.2	136.0[g]	—	−106.2		−222.5
	[−15.4]	[−20.3]	[624.0]				[14.8]

[a] In C_6D_6 (50%, v/v) at 298 K. Coupling constants ^nJ(^{119}Sn,X) (X = ^{13}C, ±0.5 Hz; X = ^{15}N, ±0.1 Hz) are given in square brackets, ^nJ(^{29}Si,X) in parentheses and ^nJ(^{207}Pb,X) in braces (X = ^{13}C, ±0.5 Hz; X = ^{15}N, ±0.1 Hz).

[b] Isotope-induced chemical shifts in parts per billion (±2 ppb); a negative sign indicates that the heavier isotopomer resonates to low frequency with respect to the lighter isotopomer.

[c] δ^{29}Si [^1J(^{29}Si,^{15}N)]; $^1\Delta$ $^{14/15}$N(^{29}Si) (±1 ppb).

[d] ^1J(^{15}N,^{13}C) = 8.7 Hz; $^1\Delta$ $^{12/13}$C(^{15}N) = −21 ± 2 ppb.

[e] δ^{107}Pb {^1J(^{107}Pb,^{15}N)}; $^1\Delta$ $^{14/15}$N(^{107}Pb) (±5 ppb).

[f] δ^{13}C = 138.7 [−38.5] (C_i); 128.6 [15.6] (C_o); 127.5 [31.0] (C_m) 124.5 [20.0] (C_p).

[g] δ^{13}C = 137.0 [45.0] (C_o); 129.5 [61.7] (C_m); 130.7 [12.8] (C_p).

the Hahn-echo extended (HEED)[7] refocused INEPT[10] pulse sequence with ^{1}H decoupling. The major part of the induced transverse magnetization responsible for the broad parent signal of the ^{14}N–^{119}Sn isotopomer decays during the Hahn-echo delay time as a result of scalar relaxation of the second kind,[11] whereas the transverse magnetization of the ^{15}N–^{119}Sn isotopomer is hardly affected (see Figs 1 and 2). These experiments also give the isotope-induced chemical shifts $^1\Delta^{14/15}$N(^{119}Sn) with ^{15}N at natural abundance.

Determination of signs of coupling constants ^1J(^{119}Sn,^{15}N), ^nJ(^{119}Sn,^{13}C) and ^{n+1}J(^{119}Sn,^{1}H)

The determination of absolute signs of coupling constants is most readily achieved by 1D or 2D experiments designed for the comparison of relative signs of coupling constants. If one or more of such experiments include so-called key coupling constants for which the absolute sign is known [e.g. $^1J(^{13}C,^1H) > 0$[12] or $^2J(^{119}Sn,^1H_{me}) > 0$ with few and rather special

Table 2. ^{13}C, ^{15}N and ^{119}Sn NMR data[a] for *N*-indolyltin derivatives 2a–d

	δ^{13}C										
No.	C(2)	C(3)	C(3a)	C(4)	C(5)	C(6)[b]	C(7)	C(7a)	δ^{119}Sn	$^1\Delta$[c]	δ^{15}N
2a[d]	131.6	103.7	131.7	121.1	120.9	119.1	112.8	142.9	73.1	−50.8	−240.5
	[8.5]	[14.2]	[12.6]				[8.0]	[7.0]			[45.3]
2b[e]	132.3	103.9	131.6	121.0	121.0	119.2	112.9	143.5	53.9	−52.8	−243.2
	[8.6]	[11.2]	[10.0]								[78.4]
2c[f]	133.9	104.2	131.6	121.0	120.6	119.3	114.7	143.5	−38.3	−80.5	−240.8
		[6.7]	[7.4]								[143.1]
2d[d]	142.5	103.4	132.3	120.0	119.8	118.9	112.4	144.2	64.3	−52.5	−239.3
	[8.6]	[11.6]	[15.6]				[8.0]	[8.9]			[40.4]

[a] In C_6D_6 (50%, v/v) at 298 K. Coupling constants ^nJ(^{119}Sn,X) (X = ^{13}C, ±0.5 Hz; X = ^{15}N, ±0.1 Hz) are given in square brackets.

[b] Without assignment.

[c] $^1\Delta^{14/15}$N(^{119}Sn) isotope-induced chemical shifts in parts per billion (±2 ppb); a negative sign indicates that the heavier isotopomer resonates to low frequency with respect to the lighter isotopomer.

[d] δ^{13}C (**2a**) = −5.6 [393.7] ($SnMe_3$); δ^{13}C (**2d**) = −3.9 [392.1] ($SnMe_3$); 16.8 [6.6] (Me).

[e] δ^{13}C (**2b**) = 5.0 [369.5], 10.2 [25.2] ($SnEt_3$).

[f] δ^{13}C (**2c**) = 36.2 [336.1], 32.1 [<2] (Sn^tBu_3).

Table 3. ^{13}C, ^{15}N and ^{119}Sn NMR data[a] for the N-carbazolyltin derivative 3

	$\delta^{13}C$								
C(1a)	C(1)	C(2)[b]	C(3)	C(4)[b]	C(4a)	R	$\delta^{119}Sn$	$^1\Delta$[c]	$\delta^{15}N$
147.4 [6.7]	112.6 [7.4]	125.4	118.7	120.8	126.3 [11.0]	−4.6 [391.0]	69.0	−56.6	−261.6 [48.1]

[a] In C_6D_6 (50%, v/v) at 298 K. Coupling constants $^nJ(^{119}Sn,X)$ ($X = {}^{13}C$, ±0.5 Hz; $X = {}^{15}N$, ±0.1 Hz) are given in square brackets.

[b] Without assignment.

[c] $^1\Delta\ ^{14/15}N(^{119}Sn)$ isotope-induced chemical shifts in parts per billion (±2 ppb); a negative sign indicates that the heavier isotopomer resonates to low frequency with respect to the lighter isotopomer.

exceptions[13]], other absolute signs of coupling constants become accessible. The presence of two active spins (e.g. X and ^1H) and one passive spin Y is required, and in most cases a 2D X/^1H heteronuclear shift correlation (HETCOR), either X or ^1H detected, provides a convenient way to compare the relative signs of $J(X,Y)$ and $J(Y,^1H)$. Alike signs are evident from a positive tilt of the relevant cross peaks in the 2D contour plot, whereas a negative tilt indicates opposite signs.[14] If the nuclei X and/or Y possess a negative gyromagnetic ratio γ, it is advisable to use the notation of reduced coupling constants K [e.g. $K(X,Y) = 4\pi^2 J(X,Y)(\gamma_X \gamma_Y h)^{-1}$].

In Scheme 2 various isotopomers are shown together with the relevant NMR experiment in order to compare the signs of coupling constants. In the case of **1a**, a 2D $^{15}N/^1H$ HETCOR experiment (Scheme 2, A), based on $^3J(^{15}N,Sn,C,^1H)$, proves that the signs of $^1K(^{119}Sn,^{15}N)$ and $^2K(^{119}Sn,^1H_{Me})$ are alike. Since $^2K(^{119}Sn,^1H_{Me}) < 0$ [$^2J(^{119}Sn,^1H_{Me}) > 0$], it follows that $^1K(^{119}Sn,^{15}N) < 0$ [$^1J(^{119}Sn,^{15}N) < 0$]. The data in Table 1 clearly indicate that the sign of the coupling constants $^1J(^{119}Sn,^{15}N)$ in the compounds studied will be negative, except

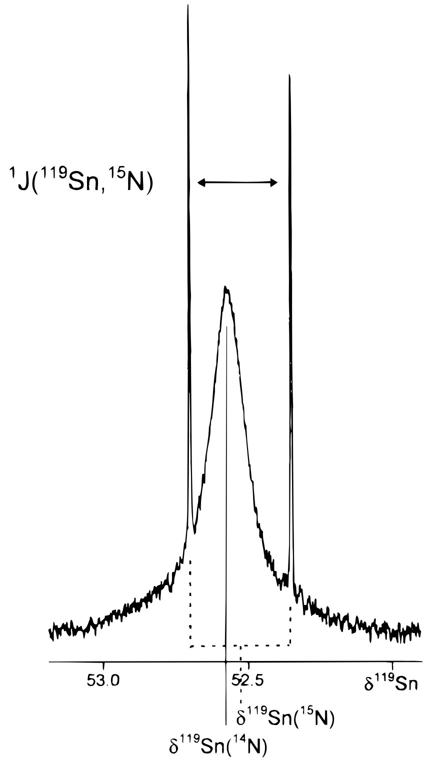

Figure 1. 186.5 MHz $^{119}Sn\{^1H\}$ NMR of **1b** (*ca.* 40%, v/v, in C_6D_6 at 25 ± 1 °C), recorded by the HEED INEPT pulse sequence. Repetition delay, 5 s; acquisition time, 3.5 s; Hahn-echo delay, 0.015 s; result of 128 transients.

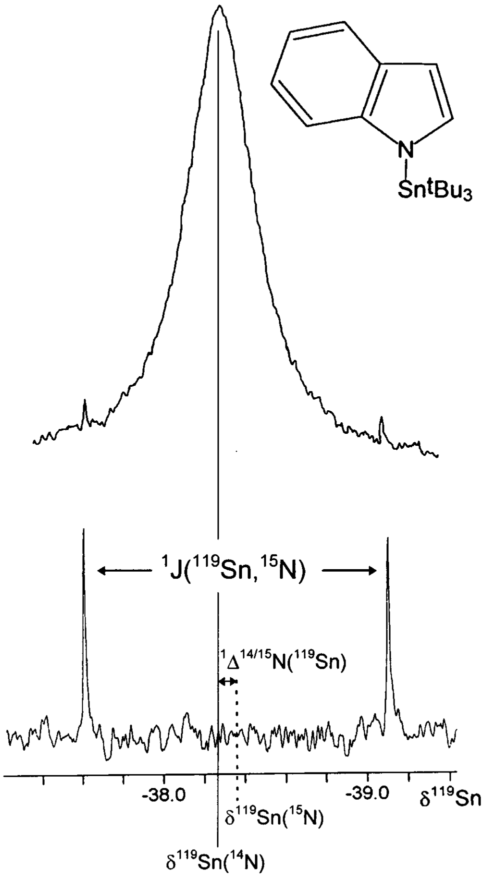

Figure 2. 93.3 MHz $^{119}Sn\{^1H\}$ NMR of **2c** (*ca.* 10% in C_6D_6, at 25 ± 1 °C), recorded by the HEED INEPT pulse sequence,[7] showing the influence of different Hahn-echo delays; 0.008 s for the upper and 0.2 s for the lower spectrum. Repetition delay, 5 s; acquisition time, 3.5 s; result of 1024 transients each.

	Isotopomers	Exp.	Coupling signs comared	Result
A	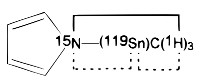	$^{15}N/^{1}H$	$\frac{{}^{2}K({}^{119}Sn,{}^{1}H)}{{}^{1}K({}^{119}Sn,{}^{15}N)} > 0$	$^{1}K(^{119}Sn,^{15}N) < 0$
B	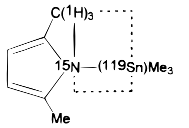	$^{15}N/^{1}H$	$\frac{{}^{4}K({}^{119}Sn,{}^{1}H)}{{}^{1}K({}^{119}Sn,{}^{15}N)} > 0$	$^{4}K(^{119}Sn,^{1}H_{Me(2,5)}) < 0$
C	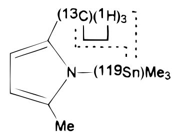	$^{13}C/^{1}H$	$\frac{{}^{4}K({}^{119}Sn,{}^{1}H)}{{}^{3}K({}^{119}Sn,{}^{13}C)} < 0$	$^{3}K(^{119}Sn,^{13}C_{Me(2,5)}) > 0$
D	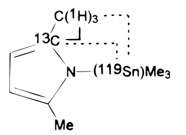	$^{13}C/^{1}H$	$\frac{{}^{4}K({}^{119}Sn,{}^{1}H)}{{}^{2}K({}^{119}Sn,{}^{13}C)} < 0$	$^{2}K(^{119}Sn,^{13}C(2,5)) > 0$
E	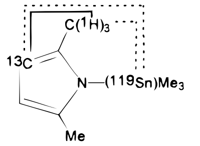	$^{13}C/^{1}H$	$\frac{{}^{4}K({}^{119}Sn,{}^{1}H)}{{}^{3}K({}^{119}Sn,{}^{13}C)} < 0$	$^{3}K(^{119}Sn,^{13}C(3,4)) > 0$
F	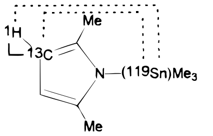	$^{13}C/^{1}H$	$\frac{{}^{4}K({}^{119}Sn,{}^{1}H)}{{}^{3}K({}^{119}Sn,{}^{13}C)} > 0$	$^{4}K(^{119}Sn,^{1}H(3,4)) > 0$
G	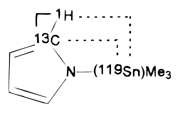	$^{13}C/^{1}H$	$\frac{{}^{3}K({}^{119}Sn,{}^{1}H)}{{}^{2}K({}^{119}Sn,{}^{13}C)} > 0$	$^{3}K(^{119}Sn,^{1}H(3,4)) > 0$

Scheme 2. Examples of isotopomers of 1a and 1d showing the active spins (either irradiated or observed; connected by a drawn line) and the passive spin (connected with the active spins by broken lines) which serve for comparing coupling signs. Owing to $\gamma(^{15}N) < 0$ and $\gamma(^{119}Sn) < 0$, the notation of reduced coupling constants is used.

in the case of **1f** where the magnitude of $^{1}J(^{119}Sn,^{15}N)$ is small (14.8 Hz) and can be of either sign. The information on the sign of $^{1}J(^{119}Sn,^{15}N)$ can be used to determine other absolute signs, as shown in Scheme 2 for **1d** as a representative example.

The various HETCOR experiments listed in Scheme 2 demonstrate that the comparison of relative coupling signs finally leads to a series of absolute signs. The magnitude of the coupling constants in **1a** and **1d**, when compared with analogous coupling constants in the other azole derivatives, suggests that there will be no changes in most of the coupling signs. A further $^{15}N/^{1}H$ HETCOR experiment (Scheme 2), this time based on $^{3}J(^{15}N,^{1}H_{Me-2,5})$, proves that the signs of $^{1}K(^{119}Sn,^{15}N)$ and $^{4}K(^{119}Sn,^{1}H_{Me-2,5})$ are alike, which means $^{4}K(^{119}Sn,^{1}H_{Me-2,5}) < 0$ $[^{4}J(^{119}Sn,^{1}H_{Me-2,5}) > 0]$ (see Fig. 3). Then various $^{13}C/^{1}H$ HETCOR experiments, based on $^{1}J(^{13}C,^{1}H)$ (e.g. for **1c** as shown in Fig. 4), $^{2}J(^{13}C,^{1}H)$ and $^{3}J(^{13}C,^{1}H)$ reveal the other missing signs of coupling constants, as listed in Scheme 2. Figures 3, 4 and 5 also show that couplings such as $^{4}J(^{119}Sn,^{1}H)$ or $^{3}J(^{119}Sn,^{1}H)$, badly resolved in the 1D ^{1}H NMR spectra, become well resolved in the 2D spectra.

$\delta^{13}C$, $\delta^{15}N$, $\delta^{119}Sn$ and isotope-induced chemical shifts

The $\delta^{13}C$ values of **1**–**3** exhibit no unusual features when compared with the parent compounds.[15] This is also true for the $\delta^{15}N$ values, although the data for the pyrrole derivatives cover a larger range than those of the indoles. Comparison of the $\delta^{119}Sn$ data for **1a**–**c** with those for **2a**–**c** shows that the parallel trend is lost for the derivatives **1c** and **2c**, pointing towards different effects due to steric crowding. It appears that in **2c** stronger interactions between the three *tert*-butyl groups and the indolyl group induces increased ^{119}Sn nuclear shielding, whereas the effect of methyl and ethyl groups attached to the tin atom is independent of the azolyl group. In the case of **2c**, the influence of steric

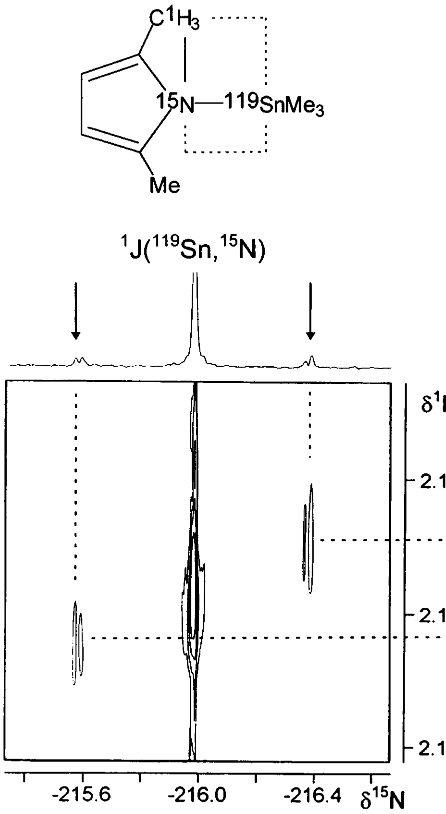

Figure 3. Contour plot of the 30.4 MHz 2D ^{15}N/^{1}H HETCOR spectrum [based on $^{3}J(^{15}\mathrm{N},^{1}\mathrm{H})$; drawn line in the formula]. The cross peaks for the ^{119}Sn satellites show a positive tilt, and therefore the signs of $^{1}K(^{119}\mathrm{Sn},^{15}\mathrm{N})$ (<0) and $^{4}K(^{119}\mathrm{Sn},^{1}\mathrm{H})$ (<0) are alike (the couplings for which the signs can be compared are indicated by broken lines in the formula).

crowding is also evident from the isotope-induced chemical shift and the coupling constants $^{1}J(^{119}\mathrm{Sn},^{15}\mathrm{N})$ and $^{1}J(^{119}\mathrm{Sn},^{13}\mathrm{C})$ (see below).

Some $^{1}\Delta^{14/15}\mathrm{N}(^{119}\mathrm{Sn})$ data have been measured, most of them by HEED experiments.[7,16] However, the present data allow for the first time a comparison between $^{1}\Delta^{14/15}\mathrm{N}(^{119}\mathrm{Sn})$, $^{1}\Delta^{14/15}\mathrm{N}(^{29}\mathrm{Si})$ and $^{1}\Delta^{14/15}\mathrm{N}(^{207}\mathrm{Pb})$ for the same type of compound [**1d**, **1d(Si)** and **1d(Pb)**], and it seems that a relationship emerges between the magnitude of $^{1}\Delta^{14/15}\mathrm{N}(^{119}\mathrm{Sn})$ and steric crowding. In the series **1d**, **1d(Si)** and **1d(Pb)**, the changes in the $^{1}\Delta^{14/15}\mathrm{N}$ values correspond approximately to the changes in the respective radial expansion terms, i.e. to the ratio of chemical shift ranges.[17] Inspection of the $^{1}\Delta^{14/15}\mathrm{N}(^{119}\mathrm{Sn})$ data for the pyrrole derivatives shows the smallest negative value for **1a** and the largest negative value for **1c**. Similarly, the $^{1}\Delta^{14/15}\mathrm{N}(^{119}\mathrm{Sn})$ value for **1d** is significantly more negative than that for **1a**. These effects become more pronounced in the series of indoles **2a**–**c** with the largest negative $^{1}\Delta^{14/15}\mathrm{N}(^{119}\mathrm{Sn})$ value for **2c** where steric crowding is most effective. Unfortunately, our attempts at the synthesis of the corresponding *N*-carbazolyl derivative were not successful. If one compares the $^{1}\Delta^{14/15}\mathrm{N}(^{119}\mathrm{Sn})$ values for the series **1a** (-38.0), **2a**

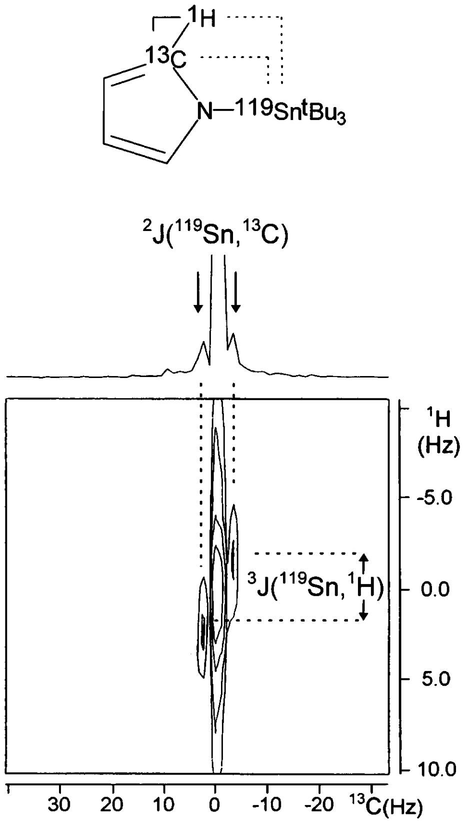

Figure 4. Contour plot of the 125.8 MHz 2D ^{13}C/^{1}H HETCOR spectrum of **1c** [based on $^{1}J(^{13}\mathrm{C},^{1}\mathrm{H})$] showing the region of the ^{13}C(2, 5) resonance. The cross peaks for the ^{119}Sn satellites are marked, and the positive tilt indicates that the signs of $^{2}J[^{119}\mathrm{Sn},^{13}\mathrm{C}(2,5)]$ are $^{3}J[^{119}\mathrm{Sn},^{1}\mathrm{H}(2,5)]$ are alike.

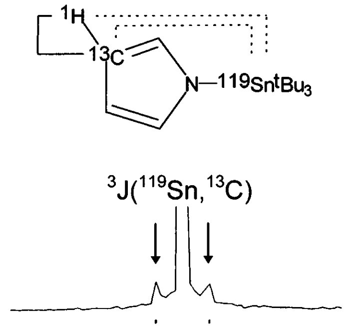

Figure 5. Contour plot of the 125.8 MHz 2D ^{13}C/^{1}H HETCOR spectrum of **1c** [based on $^{1}J(^{13}\mathrm{C},^{1}\mathrm{H})$] showing the region of the ^{13}C(3,4) resonance. The cross peaks for the ^{119}Sn satellites are marked, and the positive tilt indicates that the signs of $^{3}J[^{119}\mathrm{Sn},\ ^{13}\mathrm{C}(3,4)]$ and $^{4}J[^{119}\mathrm{Sn},\ ^{1}\mathrm{H}(3,4)]$ are alike.

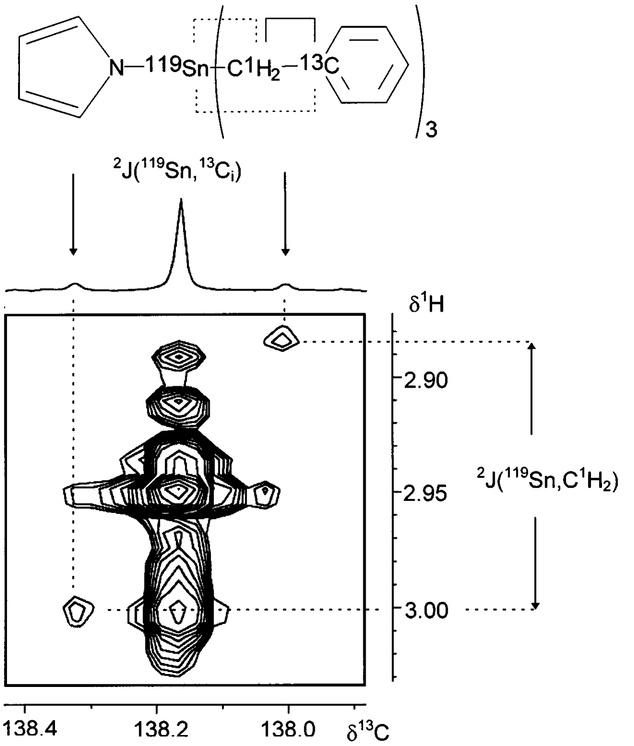

Figure 6. Contour plot of the 125.8 MHz 2D $^{13}C/^1H$ HETCOR spectrum of **1c** [based on $^2J(^{13}C,^1H)$ as indicated by the drawn line in the formula] showing the region of the $^{13}C_i$ resonance. The cross peaks for the ^{119}Sn satellites are marked, and the positive tilt indicates that the signs of $^2K(^{119}Sn,^{13}C_i)$ and $^2K[^{119}Sn,^1H(CH_2)]$ (<0) are alike.

(−50.8) and **3** (−56.6), increasing negative contributions as a result of steric crowding also become obvious.

Coupling constants $^1J(^{119}Sn,^{15}N)$ and $^nJ(^{119}Sn,^{13}C)$

On the basis of the experimentally determined negative signs of $^1J(^{119}Sn,^{15}N)$ in **1a–d**, all other coupling constants $^1J(^{119}Sn,^{15}N)$ for **1–3** should have a negative sign [$^1K(^{119}Sn,^{15}N) < 0$!], with the possible exception of **1f**. In contrast, the sign of $^1J(^{29}Si,^{15}N)$ is positive [$^1K(^{29}Si,^{15}N) > 0$] in **1d(Si)** since it is of the same magnitude as in **1a(Si)** where it has been determined experimentally.[7] The increasing polarity of the M–N bond (for M = Si, Sn, Pb) is a major reason for the large and positive value of $^1J(^{207}Pb,^{15}N)$ in **1d(Pb)** [$^1K(^{207}Pb,^{15}N) < 0$!], typical of organolead–nitrogen compounds.[8,18] Comparison of the $^1J(^{119}Sn,^{15}N)$ data for **1a** and **1d** shows that the 2,5-dimethyl-*N*-pyrrolyl group causes a slightly less polarizable Sn—N bond than the *N*-pyrrolyl group, compensating for negative contributions arising from steric repulsion. The same trend is found for **2a** and **2d**. The presence of more electronegative organyl groups at the tin atom leads, as expected, to less negative contributions to the magnitude of $^1J(^{119}Sn,^{15}N)$, as is evident in the case of **1f** [$^1J(^{119}Sn,^{15}N) = \pm 14.8$ Hz]. The presence of ethyl instead of methyl groups at the tin atom causes increased polarizability of the Sn—N bond both in **1b** [$^1J(^{119}Sn,^{15}N) = -66.5$ Hz] and **2b** [$^1J(^{119}Sn,^{15}N) = -78.4$ Hz] as compared with **1a** [$^1J(^{119}Sn,^{15}N) = -37.2$ Hz] or **2a** [$^1J(^{119}Sn,^{15}N) = -45.3$ Hz], and this is reflected by larger negative contributions to $^1J(^{119}Sn,^{15}N)$. The analogous effect of three *tert*-butyl groups at the tin atom is striking, already for **1c** [$^1J(^{119}Sn,^{15}N) = -99.9$ Hz], and particularly for **2c** [$^1J(^{119}Sn,^{15}N) = -143.1$ Hz]. It is therefore concluded that the effect of the *tert*-butyl groups, clearly evident for **1c**, is further enhanced by stronger steric interactions as in **2c** [see also the discussion of $\delta^{119}Sn$ and $^1\Delta^{14/15}N(^{119}Sn)$ values].

The increase in the magnitude of $|^1J(^{119}Sn,^{13}C)|$ with respect to the respective tetraorganotin compounds is expected, considering the electronegativity of the azolyl groups and the concept of rehybridization.[19] In the case of **2c**, when compared with **1c**, one finds again [see the $^1J(^{119}Sn,^{15}N)$ values] an appreciable change in the magnitude of $|^1J(^{119}Sn,^{13}C)|$. The smaller value for **2c** [$|^1J(^{119}Sn,^{13}C)| = 336.1$ Hz] indicate the presence of steric effects. The values $^2J[^{119}Sn,^{13}C(2,5)]$ and $^3J[^{119}Sn,^{13}C(3,4)]$ in the pyrrole derivatives **1a–c** vary in a systematic way, as can now be stated knowing the sign of these coupling constants. To the best of our knowledge, the sign of $^2J(^{119}Sn,^{13}C_i)$ in benzyltin compounds has not been determined. As shown in Fig. 6, the sign is positive, in agreement with the signs of many other geminal ^{119}Sn–element couplings for a coupling pathway across an aliphatic carbon.[9]

EXPERIMENTAL

All compounds were synthesized and handled under a nitrogen atmosphere, using carefully dried glassware and dry solvents. Electron ionization (EI) mass spectra (70 eV) were recorded using a Varian MAT CH 7 spectrometer with direct inlet. NMR spectra were measured using Bruker ARX 250, AC 300 and AM 500 spectrometers. Chemical shifts are referred to Me_4Si [δ^1H $(C_6D_5H) = 7.15$, $\delta^{13}C$ $(C_6D_6) = 128.0$, $\delta^{29}Si = 0$ for $\Xi(^{29}Si) = 19.867184$ MHz], neat $MeNO_2$ [$\delta^{15}N = 0$ for $\Xi(^{15}N) = 10.136767$ MHz], Me_4Sn [$\delta^{119}Sn = 0$ for $\Xi(^{119}Sn) = 37.290665$ MHz] and Me_4Pb [$\delta^{207}Pb = 0$ for $\Xi(^{207}Pb) = 20.290597$ MHz]. Delays for 2D heteronuclear shift correlations were optimized in the usual way by 1D polarization transfer experiments. In the case of most of the HEED experiments,[7] the Hahn-echo delay was selected in such a way that the parent signal was just visible after 16 transients. The starting materials were either commercial products [azoles, *n*-butyllithium in hexane (1.6 M), Me_3SnCl] or were prepared following literature procedures: Et_3SnCl,[20] $^tBu_3SnCl$.[21]

N-Azolyltin derivatives 1 3: General procedure

A freshly prepared suspension of the respective lithiated azole (5 mmol in 30 ml of hexane) was stirred at −78 °C and the triorganotin chloride was added in one portion. Stirring was continued for 14 h at room temperature. Then all insoluble material was filtered off and the solid material was washed with 50 ml of hexane. After removing the solvent *in vacuo*, the pure products were left in high yield (*ca.* 90%), and could be further purified either by distillation at reduced pressure or by crystallization from hexane.

1a. B.p. 105 °C/20 Torr). ^{1}H NMR (C_6D_6): δ^1H [$J(^{119}$Sn,^{1}H)] = 0.23 [+58.0] s, 9H, Me_3Sn; 6.39 [−8.5] m, 2H, H(3,4); 6.62 [−4.2] m, 2H, H(2,5).

1b. B.p. 112 °C/0.04 Torr. ^{1}H NMR (C_6D_6):δ^1H [$J(^{119}$Sn,^{1}H)] = 1.00 m, 1.08 m, 15H, Et_3Sn; 6.43 m, 2H. H(3,4); 6.67 m, H(2,5).

1c. B.p. decomp. >90 °C/0.04 Torr. ^{1}H NMR (C_6D_6):δ^1H [$J(^{119}$Sn, ^{1}H)] = 1.15 [−73.8] s, 27H, ^{t}Bu$_3$Sn; 6.49 [−3.2] m, 2H, H(3,4); 6.73 [−4.0] m, 2H, H(2,5).

1d. B.p. 72 °C/0.4 Torr. ^{1}H NMR (C_6D_6): δ^1H [$J(^{119}$Sn,^{1}H)] = 0.29 [+58.5] s, 9H, Me_3Sn; 2.16 [−2.9] s, 6H, 2,5-Me$_2$; 5.89 [−8.8] s, 2H, H(3,4).

1d(Si). B.p. 55 °C/0.4 Torr. ^{1}H NMR (C_6D_6):δ^1H [$J(^{29}$Si,^{1}H)] = 0.28 [+7.3], s, 9H, Me_3Si; 2.19 (<1.5) s, 6H, 2,5-Me$_2$; 5.83 (<2) s, 2H, H(3,4).

1d(Pb). M.p. 70–75 °C. ^{1}H NMR (C_6D_6): δ^1H [$J(^{207}$Pb,^{1}H)] = 0.98 [−70.6] s, 9H, Me_3Pb; 2.17 [<2.5] s, 6H, 2,5-Me$_2$; 5.95 [<3.0], s, 2H, H(3,4).

1e. M.p. 195–200 °C. ^{1}H NMR ($CDCl_3$): δ^1H [$J(^{119}$Sn,^{1}H)] = 2.37 [+68.5] s, 6H, PhC*H*$_2$)$_3$Sn; 6.52 m, 6H, H(*o*); 6.92 m, 6H, H(*m*); 6.83 m, 3H, H(*p*); 6.39 m, 2H, H(3,4); 6.21 m, 2H, H(2,5).

1f. M.p. 202–204 °C. ^{1}H NMR ($CDCl_3$): δ^1H [$J(^{119}$Sn,^{1}H)] = 7.72 [57.8] m, 6H, H(*o*); 7.54 [17.2] m, 6H, H(*m*); 7.56 [4.3] m, 3H, H(*p*); 6.50 [−3.3] m, 2H, H(3,4); 6.89 [−4.2] m, 2H, H(2,5).

2a. M.p. 180–185 °C. ^{1}H NMR (C_6D_6): δ^1H [$J(^{119}$Sn,^{1}H)] = 0.21 [+59.2] s, 9H, Me_3Sn; 6.83 d, 1H, H(3); 7.10 d, 1H, H(2); 7.24–7.37 m, 3H, H(5,6,7); 7.92 1H, H(4). El-MS: *m/z* (%) 281 (82) [M$^+$]; 236 (50); 165 (100) [Me_3Sn^+]; 116 (42).

2b. Oily liquid, decomp. >120 °C/0.1 Torr. ^{1}H NMR (C_6D_6): δ^1H [$J(^{119}$Sn,^{1}H)] = 0.79–1.17, m, 15H, Et_3Sn; 6.81 d, 1H, H(3), 7.10 d, 1H, H(2); 7.09–7.39 m, 3H, H(5,6,7); 7.87 m, 1H, H(4). El-MS: *m/z* (%) 323 (78) [M$^+$]; 236 (100) 116 (47).

2c. M.p. 236 °C. ^{1}H NMR (C_6D_6): δ^1H [$J(^{119}$Sn, ^{1}H)] = 1.26 [−70.0] s, 27H, ^{t}Bu$_3$Sn; 6.83 d, 1H, H(3); 7.21–7.27 m, 2H, H(5,6); 7.48 d, 1H, H(2); 7.71 m 1H, H(7); 7.85 m, 1H, H(4). El-MS: *m/z* (%) 407 (10) [M$^+$]; 350 (10); 294 (10); 236 (100); 234 (78).

2d. M.p. 30–35 °C. ^{1}H NMR (C_6D_6): δ^1H [$J(^{119}$Sn,^{1}H)] = 0.25 [+58.3] s, 9H, Me_3Sn; 2.20 [<2.5] s, 3H, 2-Me; 6.38 s, 1H, H(3); 7.13–7.27 m, 3H, H(5,6,7); 7.66 m, 1H, H(4). El-MS: *m/z* (%) 295 (54) [M$^+$]; 250 (19), 165 (88) [Me_3Sn^+]; 130 (100).

3. M.p. 64–66 °C. ^{1}H NMR (C_6D_6): δ^1H [$J(^{119}$Sn, ^{1}H)] = 0.25 [+57.2] s, 9H, Me_3Sn; 7.27–7.43 m, 6H, H(1,2,3); 8.16 m, 1H, H(4). El-MS: *m/z* (%) 331 (8) [M$^+$]; 286 (5), 165 (100) [Me_3Sn^+].

Acknowledgements

Support of this work by the Deutsche Forschungsgemeinschaft and the Fonds der Chemischen Industrie is gratefully acknowledged.

REFERENCES

1. Yu. J. Dergunov, V. F. Gerega and O. S. D'yachkovskaja, *Russ. Chem. Rev.* **46**, 1132 (1977).
2. J. G. A. Luijten and G. J. M. van der Kerk, *Recl. Trav. Chim. Pays-Bas* **82**, 1181 (1963).
3. J. C. Pommier and D. Lucas, *J. Organomet. Chem.* **57**, 139 (1973).
4. (a) R. Gassend, M. Delmas, J. C. Maire, Y. Richard and C. More, *J. Organomet. Chem.* **42**, C29 (1972); (b) R. Gassend, J. C. Maire and J. C. Pommier, *J. Organomet. Chem.* **132**, 69 (1977).
5. B. Wrackmeyer, *J. Organomet. Chem.* **297**, 265 (1985).
6. J. Hillmann, H.-D. Hausen, W. Schwarz and J. Weidlein, *Z. Anorg. Allg. Chem.* **621**, 1785 (1995).
7. E. Kupce and B. Wrackmeyer, *J. Magn. Reson.* **97**, 568 (1992).
8. B. Wrackmeyer and E. Kupce, in *Topics in Physical Organometallic Chemistry*, edited by M. Gielen, Vol 4, pp. 289–352. Freund Publishing House, Tel Aviv (1992).
9. (a) B. Wrackmeyer, *Annu. Rep. NMR Spectrosc.* **16**, 73 (1985); (b) B. Wrackmeyer, in *Physical Organometallic Chemistry—Advanced Applications of NMR to Organometallic Chemistry*, edited by M. Gielen, R. Willem and B. Wrackmeyer, Vol. 1, pp. 87–122. Wiley, Chichester (1996).
10. (a) G. A. Morris, *J. Am. Chem. Soc.* **102**, 428 (1980); (b) D. P. Burum and R. R. Ernst, *J. Magn. Reson.* **39**, 163 (1980).
11. A. Abragam, *The Principles of Nuclear Magnetism*, pp. 264–353. Oxford University Press. London (1961).
12. C. J. Jameson, in *Multinuclear NMR*, edited by J. Mason, pp. 89–131. Plenum Press, New York (1987).
13. J. D. Kennedy and W. McFarlane, *J. Chem. Soc., Chem. Commun.* 983 (1974).
14. A. Bax and R. Freeman *J. Magn. Reson.* **45**, 177 (1981).
15. H. O. Kalinowski, S. Berger and S. Braun, *^{13}C-NMR-Spektroskopie*. Georg Thieme, Stuttgart (1984).
16. B. Wrackmeyer, I. Ordung and B. Schwarze *J. Organomet. Chem.* in press.
17. (a) J. D. Kennedy, W. McFarlane and G. S. Pyne, *J. Chem. Soc., Dalton Trans.* 2332 (1977); (b) T. N. Mitchell, *J. Organomet. Chem.* **255**, 278 (1983); (c) B. Wrackmeyer, in *Unkonventionelle Wechselwirkungen in der Chemie Metallischer Elemente*, edited by B. Krebs, pp. 111–124. VCH, Weinheim (1992).
18. (a) B. Wrackmeyer and H. Zhou, *Main Group Met. Chem.* **13**, 99 (1990); (b) B. Wrackmeyer and H. Zhou, *Magn. Reson. Chem.* **28**, 1066 (1990); (c) B. Wrackmeyer, K. Horchler and H. Zhou, *Spectrochim Acta, Part A* **46**, 809 (1990).
19. H. A. Bent, *Chem. Rev.* **61**, 275 (1961).
20. K. A. Kocheskov, *Ber. Dtsch. Chem. Ges.* **66**, 1661 (1933).
21. H. H. Huang, K. M. Hui and K. K. Chiu, *J. Organomet. Chem.* **11**, 515 (1968).